Contact Angles: From Past Mistakes to New Developments through Liquid-Solid Adhesion Measurements

Jaroslaw W. Drelich
Department of Materials Science and Engineering
Michigan Technological University
Houghton, MI 49931, USA

Email: jwdrelic@mtu.edu; Phone: 1(906)4872932

Abstract

A contact angle observed for a liquid-solid system is not necessarily a unique value and a few different contact angles need to be carefully considered in relation to liquid spreading, adhesion and phase separation. Despite the conceptual simplicity of the contact angle and over 200 years of investigation, interpretations of experimental contact angles remain controversial, and mistakes are quite common. Here, the physics behind equilibrium contact angles are restated and their misuse in modern literature is briefly discussed. Selected advances made in the 20th century that shaped current interpretations of experimental contact angles are also critically reviewed and evaluated. Understanding of contact angles for liquids on solids has improved in the last two decades and this progress is driven by advanced imaging techniques and improved methodologies in contact angle measurements, often in tandem with direct force measurements for liquid droplets in contact with solids. In our laboratory, a microelectronic balance system is employed to measure the force of liquid droplet spontaneous spreading and the water-solid adhesion forces at different stages of droplet retraction and separation. A microbalance equipped with a camera and data acquisition software measures these forces directly, monitors droplet-surface separation including distances over which the droplet stretches, and collects optical images simultaneously. The images are used to analyze capillary and surface tension forces based on measured droplet dimensions, shapes of surfaces and values of contact angles. These force measurements have significantly furthered our fundamental understanding of advancing, receding and most stable contact angles, and their correlations with adhesion, and are summarized in this review.

Keywords: contact angle, liquid-solid adhesion, wetting

List of notations:

f is the fractional area or fractional line; subscripts *i, 1, 2* and *S* refer to component *i, 1, 2* and fraction of the liquid base in contact with solid surface, respectively

F is the force; subscripts *in*, *max*, and *off* refer to spreading, maximum adhesion and pull-off

ΔF is the force barrier; subscripts A and R refer to barrier between spontaneous spreading and most stable state and between most stable and pull-off states, respectively

h is the thickness of the wetting film; h_0 refers to wetting film in equilibrium with the meniscus of bulk liquid or with the sessile drop; superscripts *1* and *2* refer to films with different thicknesses

r is the roughness parameter; subscript l refers to roughness ratio of the solid that is in contact with the liquid

R is the radius of liquid droplet; subscripts *in*, *max* and *off* refer to radius after droplet spontaneous spreading, at maximum adhesion, and during pull-off separation

σ is the interfacial tension, where subscripts *SV*, *L*, and *SL* refer to solid-vapor, liquid, and solid-liquid, respectively

θ is the contact angle; superscripts *C*, *CB*, *W*, and *Y* refer to contact angles defined by Cassie, Cassie-Baxter, Wenzel, and Young equations, respectively; superscripts *1*, *2*, *A* and *R* refer to component 1, component 2, advancing and receding contact angle, respectively

$\Pi(h)$ is the disjoining pressure in the wetting film

Definitions of Contact Angles

Some of the definitions were reproduced directly from earlier publication as per referencing.

Contact angle: an angle experimentally observed on the liquid side (denser liquid side if there are two liquids) between the tangent to the solid surface and the tangent to the liquid-fluid interface at the contact line between the three phases [1].

Apparent contact angle: the contact angle measured experimentally on a macroscopic scale [1].

Advancing contact angle: the highest metastable apparent contact angle that can be measured [1].

Receding contact angle: the lowest metastable contact angle that can be measured [1].

Contact angle hysteresis: the difference between advancing and receding contact angles [1].

Equilibrium contact angle: the contact angle that corresponds to a global or local minimum of the Gibbs energy of a system, irrespective of the solid characteristics.

Metastable (equilibrium) contact angle: the contact angle pertaining to a wetting liquid trapped at an energy level (metastable state) of the system above the absolute minimum (subjected to no more than thermal fluctuation disturbances and natural vibrations).

Ideal contact angle: the contact angle on an ideal surface [1].

Young contact angle: the contact angle that is calculated from the description of the Young equation [1].

Wenzel contact angle: most stable contact angle for a rough surface used in conjunction with the Wenzel equation.

Cassie contact angle: most stable contact angle for heterogeneous solid surface used in conjunction with the Cassie equation.

Cassie-Baxter contact angle: most stable contact angle for partially wetted rough surfaces used in conjunction with the Cassie - Baxter equation.

Most stable contact angle: the apparent contact angle associated with the state of lowest Gibbs energy for a system [1].

Introduction

This review summarizes a keynote address delivered by the author for the 16th International Conference on Surface Forces that took place in Kazan (Russia) on August 20 – 25, 2018. In the first half of this contribution, key theoretical models used in interpretation of contact angles are briefly reviewed, and their misinterpretations and overuses in modern literature are highlighted. Research in the 20th century has advanced our understanding of contact angles. Nevertheless, a few misleading conclusions were drawn from theoretical and experimental works that put researchers on the wrong track with the use and analysis of contact angles. These mistakes are being corrected with major advances in modeling and interpretation of contact angles, often driven by advanced imaging capabilities and force measurements, with more still to come. Force measurements between water droplets and surfaces of solids and liquids are important contributions to this recent progress. In the second half of this review, major findings from adhesion force measurements combined with contact angle analysis for droplets at their different stages of spreading, retraction and separation are summarized and discussed. New experimental observations described in this review complement recent research results from other laboratories and are expected to contribute strongly to advances in interpretation of experimental contact angles. They also contribute to new research directions in characterization of solid surfaces and interpretation of contact angles including contact angle hysteresis. At the end, key findings and recommendations for future research work are offered.

Basic Models on Contact Angles

During partial spreading, the liquid forms a lens with a finite *contact angle* (θ) at the solid surface. The contact angle is defined as the angle between the solid surface plane and the tangent to the liquid surface plotted at the point of contact between three phases. There are four key equations that correlate *equilibrium contact angle* at lowest Gibbs energy of the system with solid surface energy/tension and other solid surface characteristics (we will return to the definition of equilibrium contact angle later). These include the Young's equation (1) for ideal solid surfaces [2], the Wenzel equation (2) that takes into account solid surface roughness [3], the Cassie equation (3) describing the case of a liquid in contact with a heterogeneous solid surface [4], and the Cassie-Baxter equation (4) for a liquid sitting on top of a textured solid surface with trapped air underneath [5]. Figure 1 shows schematics for the shapes of water on solid surfaces of different surface characteristics.

Equations (2)-(4) were originally proposed based on empirical approaches. Nevertheless, these equations can be derived using thermodynamic reasoning if appropriate assumptions are made [6].

The Young's equation is defined as:

$$cos\theta^{Y} = \frac{\sigma_{SV} - \sigma_{SL}}{\sigma_{L}} \quad (1)$$

In the case of microscopic and sub-microscopic droplets, a tension component associated with the three-phase contact line needs to be added to Young's equation [7-9].

The contact angle defined by Young's equation (1) is referred to as the *ideal contact angle* or more commonly *Young's contact angle* (θ^{Y}) and is valid only for ideal solids whose surfaces are homogeneous, isotropic, smooth, and rigid, and when surrounding fluids are inert to such a solid (no chemical reaction or specific adsorption, dissolution, swelling, or rearrangement of phases, molecules, and functional groups).

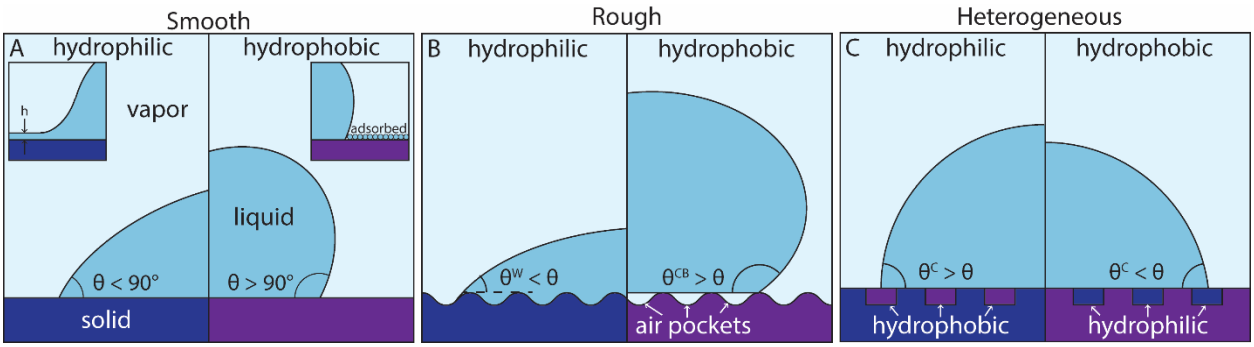

Figure 1. Schematics of water and related contact angles on smooth, rough and heterogeneous solid surfaces. The symbols include: h – thickness of a liquid film, θ – contact angle, θ^{W} – Wenzel contact angle, θ^{CB} – Cassie-Baxter contact angle, and θ^{C} – Cassie contact angle.

The Wenzel equation (2) applies to similar solids as Young's equation with exception of smoothness. This model takes into account a surface roughness that is penetrable by the wetting liquid but does not produce any local capillarity effects.

$$cos\theta^{W} = rcos\theta^{Y} \quad (2)$$

The Cassie equation (3) for two-component (smooth) heterogeneous surface is:

$$cos\theta^{C} = f_1 cos\theta_1^{Y} + f_2 cos\theta_2^{Y} \quad (3)$$

which can be generalized to a multi-component heterogeneity as follows:

$$cos\theta^{C} = \sum_i f_i cos\theta_i^{Y} \quad (3a)$$

Heterogeneities must form separate phases/domains with their own surface characteristics, and their sizes need to be two or more orders of magnitude smaller than dimensions of the liquid droplet base (dimensions of the three-phase contact line) during contact angle measurements to satisfy the Cassie equation. Other restrictions are as for Young's equation.

If the surface is rough, the Cassie equation can be combined with the Wenzel equation as follows:

$$cos\theta^{CW} = \sum_i r_i f_i cos\theta_i^Y \quad (3b)$$

The specific case of liquid wetting a porous surface is defined by a modified Cassie equation that has been named the Cassie-Baxter equation (4) [5]:

$$cos\theta^{CB} = f_1 cos\theta^Y - f_2 \quad (4)$$

where f_1 and f_2 according to Cassie and Baxter are the total area of solid-liquid interface and liquid-air interface, respectively, *in a plane geometrical area of unity parallel to the rough surface*. This equation has been adopted for a liquid sitting on top of asperities/posts of any rough/structured surface and predicts an apparent contact angle for any geometry and structure of the surface, the topography of which is not fully penetrated by wetting liquid, also known as "heterogeneous wetting." Because f_1 is also dependent on solid surface topography, it should be emphasized that $f_1 + f_2$ can be larger than 1, a fact that was shown in the original paper but is often ignored in many modern publications. Marmur analyzed the case of liquid covering a fabric made of rounded fibers or sitting on posts that are not flat, and concluded that the Cassie-Baxter equation requires the addition of a roughness factor (r_l) and can be expressed as [10]:

$$cos\theta^{CB} = r_l f_S cos\theta^Y - (1 - f_S) \quad (4a)$$

where f_S is the fraction of the projected area of the solid surface that is wetted by the liquid.

All three models, equations (2)-(4), serve as good approximations only when the roughness and heterogeneity sizes are sufficiently small relative to the drop size used in contact angle measurements and theoretical modeling [11, 12].

A practical challenge for heterogeneous and rough systems is always to define and quantify the values of f, f_i, and f_S. Although determination of roughness factor appears straightforward, with current instruments such as atomic force microscopy, it is still debatable whether the approach proposed by Wenzel is accurate [11]. Knowing the f and r values in equations (2)-(4) allows the Young contact angle to be determined, assuming that the three-phase system is in its lowest Gibbs energy state during measurements of equilibrium contact angles on rough and/or heterogeneous surface. Additional requirements are that the size of a liquid drop used in contact angle measurements is at least three orders of magnitude larger than surface roughness and heterogeneity features and the drop maintains its axisymmetric shape [13].

There is also fifth important thermodynamic equation derived by Derjaguin [14], which describes the Young contact angle (θ^Y) in relation to the isotherm of *disjoining pressure* $\Pi(h)$ that takes into account contributions from surface forces:

$$\sigma_{LV} cos\theta^Y = \sigma_{LV} + \Pi(h_0)h_0 + \int_{h_0}^{\infty} \Pi(h)dh \quad (5)$$

For the most recent analysis of surface forces in wetting see Ref. [9]. Because the Derjaguin model relies on isotherms of disjoining pressures for thin liquid films, it is a more challenging model for analysis of practical systems than the other models described earlier.

Over-interpretation of Thermodynamic Models

The contact angle is conveniently measured at a macro scale through optical means and commonly reported in the modern literature, as a simplistic way to describe wetting characteristic of a solid and analyze liquid behavior on it. Unfortunately, as emphasized many times in the past, solids examined in research laboratories and conditions of contact angle measurements described in the modern literature deviate significantly from ideal cases posed by the assumptions used in derivation of equations (1) to (4). The ideal solids do not exist; although many solids are inert to

liquids, rigid, and can be prepared with clean surfaces, they are rough at atomic or molecular levels. Additionally, they are often not at chemical or phase equilibria during contact angle measurements. For example, liquids like water tend to evaporate and adsorb on dry solid surfaces, changing their solid surface energy [15]. The problems with solid surface quality, rigidity and contamination, and lack of equilibrium conditions, were already mentioned many times in the past [16, 17] and will not be repeated here.

The contact angle varies along the three-phase contact line for a liquid drop resting on a rough and/or heterogeneous solid surface. As theoretically proven, locally, the actual contact angles are equal to Young contact angles if the system is at equilibrium [18, 19]. Local changes in angles are due to changes in inclination of the rough surface [20] and variation in chemistry of a heterogeneous surface [21] (cause the three-phase contact line to contort). Since the contact angles are typically measured macroscopically for liquid drops with a diameter of a few millimeters using low-magnification optical lenses, the local angles are not recorded. Instead, the global contact angles are measured and are referred to as *apparent contact angles*. A liquid in contact with a real solid surface has more than one apparent contact angle [20, 21].

As shown in Figure 2, the Gibbs energy vs. apparent contact angle curves have multiple minima for a liquid on a heterogeneous and/or rough solid surface, in contrast to the curve for a smooth and homogeneous solid surface with only a single minimum [11, 22]. The liquid can be trapped in one of the metastable or stable states and each energy minimum defines a stable geometry of the liquid, with a unique equilibrium contact angle that can be measured experimentally. The advancing and receding contact angles are *metastable equilibrium contact angles* since these contact angles typically may relax to different values after mechanical stimuli are imposed on the system. Experimental advancing and receding contact angles are highest and lowest contact angles, respectively, for which there exists a local minimum in the Gibbs energy curve (Figure 2) that the liquid cannot escape from employing natural vibrations [13]. *Most stable contact angle* corresponds to the lowest Gibbs energy for a system under consideration. This new term was introduced more recently to differentiate from an equilibrium contact angle, which has a much broader meaning and can also refer to equilibrium values at metastable states (see ref. [13] for complete discussion of equilibrium and most stable contact angles). Some authors have used this new term to describe a contact angle that is experimentally accessible after mechanical stimuli are applied to the system and force the liquid to relax to the most stable mechanical configuration [23, 24]. Both definitions are correct but it still remains to be verified whether experimental most stable contact angles are always associated with the lowest Gibbs energy.

Since the beginning of the 20th century, it has been broadly accepted that both *advancing* and *receding* contact angles should be measured and reported. Since the 1960s, the advancing contact angle is considered as the maximum metastable contact angle measured for the liquid drop that advances or recently advanced over an unwetted solid surface under particular natural vibrations. The receding contact angle is the minimum metastable contact angle measured for the liquid receding or recently retreated from the wetted solid under natural vibrations. The experimental protocol for measurements of advancing and receding contact angles was published earlier [25] (Huhtamaki et al. [26] recently updated this protocol with additional practical tips related to modern drop shape profiling software).

Because contact angle measurements are among the simplest and most commonly used surface characterization methods, nowadays researchers with diverse backgrounds representing almost all fields of science and engineering use these methods, not always with sufficient training in preparation of surfaces and measurement of contact angles or their interpretation [17]. As a result, the modern literature is also flooded with “static” contact angles that are in between advancing and

receding and are neither at lowest energy state nor equilibrium with their surroundings, making the use of equations (1)-(4) improper [1]. Additionally, reproduction of these experimental "intermediate" contact angles, if pursued, becomes a challenge to other laboratories. The problem of questionable contact angle measurement methodologies was raised in an earlier publication [1], and recommendations on sample preparation and contact angle measurements protocols were made [25]; these will not be repeated here.

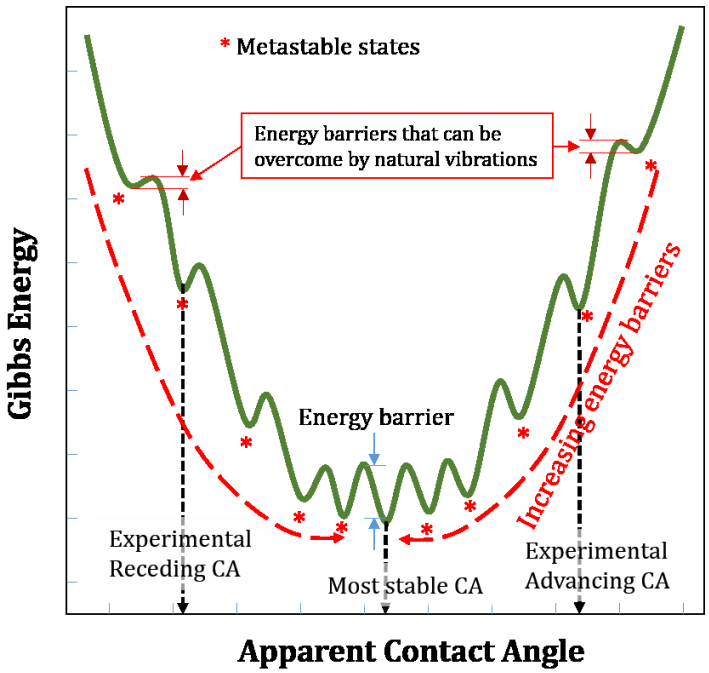

Figure 2. The Gibbs energy for a liquid on a heterogeneous and/or rough solid surface in relation to apparent contact angle. Based on Ref. [13]. CA stands for contact angle.

Neither advancing nor receding nor static contact angles should be used in conjunction with Young's, Wenzel, Cassie, and Cassie-Baxter equations. These theoretical equations describe *equilibrium contact angles* associated with the lowest Gibbs energy of a liquid on either idealized smooth or rough surfaces (referred to as the *most stable contact angles* in this contribution). The equilibrium contact angle in this review refers to a contact angle measured at minimum Gibbs energy and at metastable states as recommended by Marmur [27]. The advancing and receding contact angles are *metastable contact angles* since these contact angles typically relax to different values over longer times during the phase equilibration process [28-31] and after introducing mechanical stimuli [23, 32-34]. Only contact angles that have relaxed to the most stable state can be used in conjunction with equations (1)-(4), as per earlier recommendations [13, 35].

Unfortunately, equations (1)-(4) are typically accepted *a priori* in almost every review and research paper published over the last few decades, even if discussions in these papers often refer to real solid surfaces on which only advancing, receding or static contact angles were measured. Selection and measurement of meaningful contact angles is still challenging, especially on rough and structured surfaces [36]. The lack of measurements of contact angles when the liquid reaches the lowest energy state hinders experimental judgment of theoretical models. Despite it being a belief of the last 50 years, experimentally measured advancing and receding contact angles are generally

not representative of what thermodynamic relationships predict, a fact that is often not well recognized by the users and critics of contact angles or models.

Contact Angle Hysteresis

When two surfaces of immiscible and inert phases are brought together they interact with each other through physical adhesion. The work done on combining and separating these surfaces would be the same for ideal phases under ideal equilibrium conditions [37]. In real systems, both adhesion hysteresis for solid – solid systems and contact angle hysteresis for liquid on solid reflect deviations from idealized systems and conditions, typically encountered in thermodynamic analyzes such as represented by equations (1)-(5). Adhesion hysteresis was studied in detail in the past [37] and will not be discussed here.

Hysteresis of contact angles is a commonly studied and reported value in contact angle measurements and wetting/dewetting phenomena. In general, the advancing contact angle measured for a liquid that spreads over a dry surface is larger than receding contact angle measured for a liquid that retreats from a wet surface, and the difference is called *contact angle hysteresis*. Both advancing and receding contact angles are typically measured in the first several seconds-to-a minute time interval after a change in liquid-solid coverage area [25]. This practice has been adopted for a few decades due to its simplicity, time effectiveness and convenience. System relaxation and benefits associated with its examination are not recognized by many researchers. A liquid kept on a solid surface in a closed compartment, under closed system conditions, for hours to days (depending on the system) can produce relaxed contact angles that might reflect values of most stable contact angles or close to them [28, 29].

Despite tremendous advances in both theoretical analysis and experimental methods since the 1960s, contact angle hysteresis remains poorly understood and mostly unpredictable for a variety of liquids on a variety of solids (or liquids) [38]. As of today, contact angle hysteresis is mainly attributed to surface heterogeneity [22, 39, 40] and roughness [20, 41, 42] (Figure 3B&3C), acting as sources of contact line pinning, which magnitute depends on history of liquid motion [43]. It can also be caused by intrinsic mechanical instability of a deformable solid [44-48] (see insert in Figure 3A). Polymers and other organic specimens demonstrate surface chemical irreversibility during the time of contact angle measurements that is associated with reorganization, realignment, and diffusion of polar functionalities [30, 49, 50] (Figure 3D), which contribute to hysteresis and its time dependency as well. Additionally, contact angle hysteresis can result from different disjoining pressure for a liquid film that extends beyond a perimeter of spreading and retreating liquid [9, 51, 52] (Figure 3E). Reports on contact angle measurements for nearly ideal surfaces (smooth, homogeneous, inert and non-deformable surfaces) [30, 31, 53] are rare but the likelihood of contact angle hysteresis on such surfaces is under consideration [31, 51, 54, 55].

Misconceptions Introduced in the Middle of the 20th Century

Fixed and invariable contact angles were measured and reported throughout the 19th century until the first few years of the 20th century [56]. As early as 1890, Lord Rayleigh reported that he observed more than one stable contact angle on a solid surface [57]: "*The angles recorded* (between water and glass) *are maximum angles. If after a drop has been deposited some of the liquid is drawn off, the angle may be diminished almost to zero*." This note was ignored at first. Advancing and receding contact angles, or alternatively, angles measured with the sessile-drop and captive-bubble methods, were reported from the beginning of the 20th century. It was, however, not until the 1960s

and 70s, when the effects of solid surface heterogeneity and roughness on contact angles received more methodical investigations.

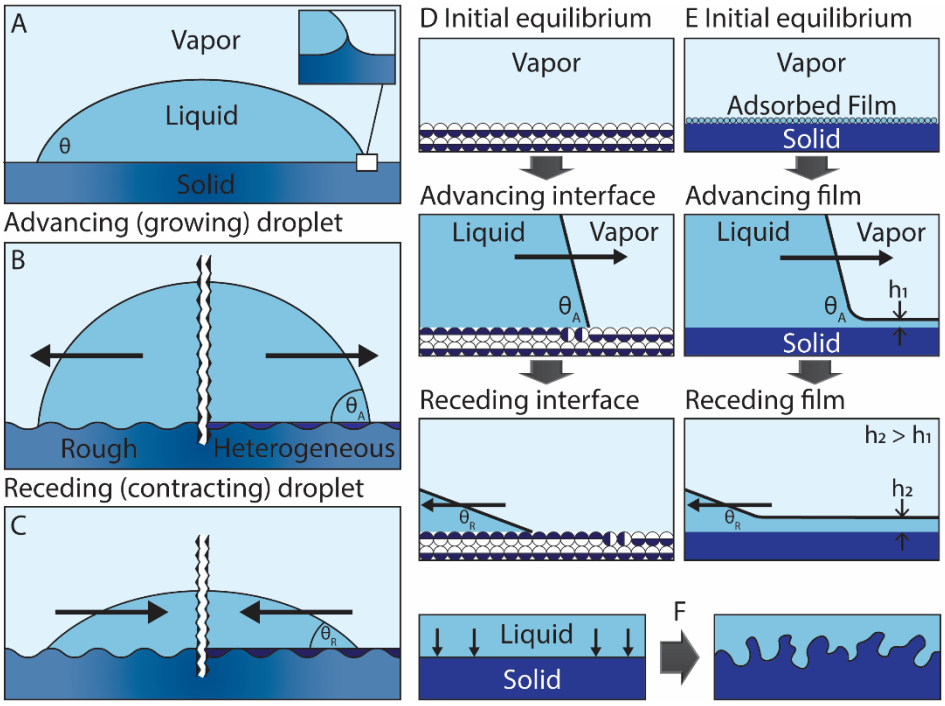

Figure 3. Schematics of liquid droplets on solids of varying surface characteristics and contact angle hysteresis. A) Liquid droplet resting on a flat solid surface. Insert: elastic and/or plastic deformation under three-phase contact line caused by normal liquid stress ($\gamma_{LV}\sin\theta$) and balanced by local stresses on the solid. B) and C) Contact angle hysteresis caused by solid surface roughness (left side) and heterogeneity (right side). D) A difference in affinity of solid chemistry to non-polar gas and polar liquid phases as a cause of contact angle hysteresis. E) Thin liquid film formed during liquid retreat can be thicker from precursor film formed during spreading. Contact angle hysteresis is caused by different disjoining pressure. F) Roughening of smooth and homogeneous surface by swelling. Symbols include: h – thickness of a liquid film, θ – contact angle, θ_A – advancing contact angle, and θ_R – receding contact angle.

The work of Johnson and Dettre [39, 41, 58-60], and then Neumann and Good [20, 21] shed a new light on contact angles for liquids on imperfect surfaces. Unfortunately these works also sparked misleading conclusions that shaped the modern interpretation of contact angles and their use in characterization of solid surfaces. For example, following the work by Johnson and Dettre [59, 60], Figure 3 shows two graphs that summarize correlations between contact angles and heterogeneity of either hydrophobic or hydrophilic surfaces.

As per Figure 4 (case 1), an advancing water contact angle measured on a hydrophobic surface contaminated with hydrophilic inclusions is only slightly affected by amount of inclusions until they cover a significant portion of the hydrophobic surface. On the contrary, even small quantities of hydrophilic inclusions can cause pinning of the water edge during its retreating. In the case of a

hydrophilic surface decorated with hydrophobic inclusions (Figure 4, case 2) the situation is quite similar. Here the advancing water contact angle rises to a high value very quickly when the hydrophilic surface is only slightly decorated with hydrophobic inclusions and remains only slightly affected with increasing fraction of surface covered by hydrophobic component. Receding contact angle, on the other hand, remains at a very low value until a significant portion of hydrophilic surface is covered with hydrophobic inclusions.

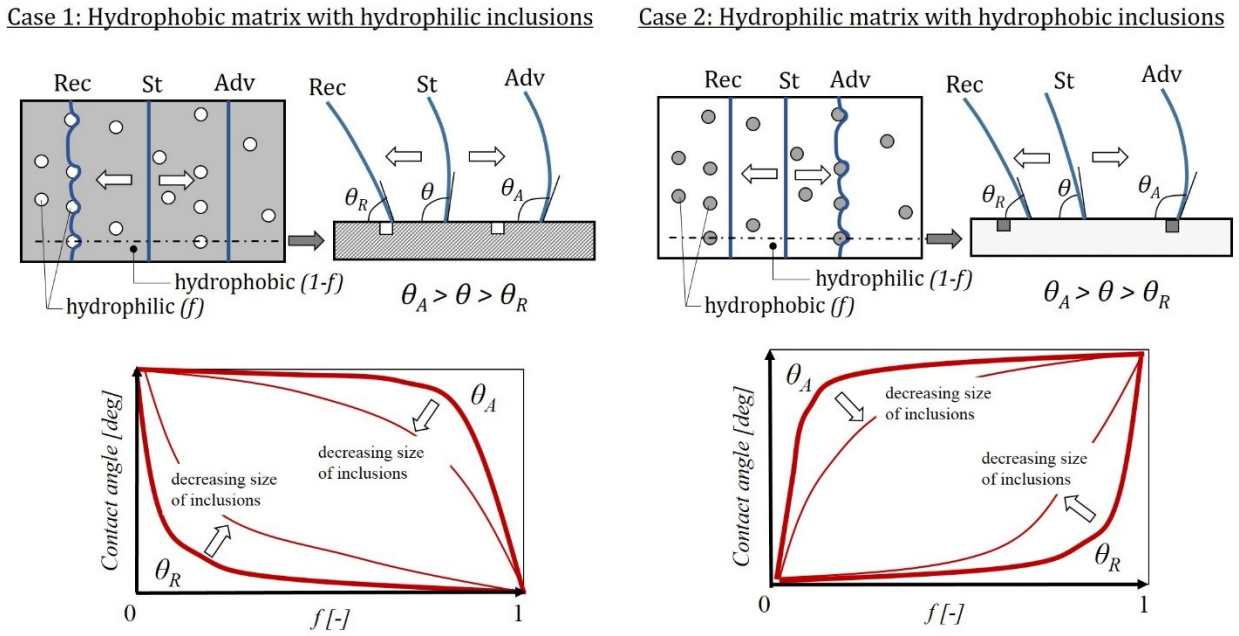

Figure 4. Effect of surface heterogeneity on characteristic of three-phase contact line and contact angle. The graphs present correlations between advancing and receding contact angles and fractional area of solid covered by inclusions (heterogeneity). *Rec*, *St*, *Adv* stand for receding, static and advancing contact line, respectively; θ_R, θ, and θ_A refer to receding, static and advancing contact angles, respectively.

These graphs, generated in the 1960s led to a belief that advancing contact angle describes the hydrophobic component of solid surface and receding hydrophilic component. Two selected quotations from publications tell the rest of the story [61]: *"The equilibrium angle on the lower-free energy areas of the surface is the maximum value that the advancing angle can take on, and the equilibrium angle on the higher-energy areas is the lowest retreating angle that is observable,"* and [62]:*"…the advancing contact angle is thermodynamically significant and can be used in Young's equation."* Although both statements can be correct under certain experimental conditions, they cannot be applied to advancing and receding contact angles measured using commonly-accepted protocols such as those described in [25]. From the 1960s until now, advancing contact angles have been mistakenly used in characterization of solid surfaces and their surface free energy using a number of theoretical and empirical models [62]. This will need to be corrected in the near future, and likely most stable contact angles will replace advancing contact angles.

Additionally, the free energy calculations for a liquid on heterogeneous and rough surfaces carried out by Neumann, Good and others led to a value of 100 nm as a first estimate of the critical size for

surface imperfection contribution to contact angle hysteresis [20, 21]. The lateral dimension of <100 nm became a benchmark target in specimen fabrication, polishing and cleaning procedures for many years. This was another example of conclusions from overall very useful theoretical analysis being over-stated. It should be recognized that free energy calculations are limited to determination of a difference between initial and final energetic states, without paying any attention to time necessary to reach the energy minimum. Such analysis also often ignores the number and values of energy barriers that need to be passed by liquid between energetic states. In experimentation, both advancing and receding contact angles are typically measured in the first several seconds after changes are imposed on liquid shape and/or volume. Equilibration time, during which the solid surface is saturated by liquid vapors and the system relaxes to a more stable state (in many cases likely to the most stable state but this will need to be validated), can take anywhere from hours to days, depending on quality of the solid surface and its saturation with liquid vapors [28]. During such equilibration a thin liquid film often stabilizes on the solid surface around the liquid contact line [9]. Unfortunately, contact angle relaxation measurements are scarce in the technical literature [28, 29], despite the fact that equilibrated/stable contact angles are a valuable addition to both advancing and receding contact angles routinely measured these days in many laboratories. One drawback of equilibration is that polymers and self-assembled monolayers tend to reorient their structures and functional groups during prolonged contact with liquid [30, 49, 50], which further complicates interpretation of contact angle values.

At present, very little is known about contact angles measured at the single states of system equilibrium that satisfies the second law of thermodynamics. Nevertheless, starting from the 1990s, attempts have been made to measure the most stable contact angles as briefly described in the next section and continued later.

(Selected) Improvements of Recent Years

Experimental Stable Contact Angles

The phenomenon of multiple liquid-solid metastable configurations can be analyzed in terms of the Gibbs energy that takes into account details of surface geometry, topography and local wettability. Figure 2, presented earlier, shows a correlation between Gibbs energy and apparent contact angle for a liquid on a heterogeneous solid surface. Similar graphs could be drawn for a rough surface.

The correlations between Gibbs energy and apparent contact angle for a liquid spreading over either rough or heterogeneous surfaces or both have been known since the 1960s. They are commonly used to demonstrate metastable states of liquid on imperfect solids and help to carry out a qualitative interpretation of contact angle and contact angle hysteresis. Already in 1969, Johnson and Dettre made the following important suggestion [59]: *the advancing and receding contact angles might converge to a common value if sufficient energy were supplied to overcome the energy barriers between the metastable states*. This suggestion was poorly explored until the 1990s. By introducing extra external energy through mechanical vibrations during contact angle measurements, researchers observed and reported relaxation of liquid on a solid surface to a more stable state at or around lowest system energy [32, 63, 64]. Installation of speakers and replacement of mechanical means with acoustic vibrations was introduced in the 21st century [33, 34, 65, 66]. It was demonstrated that external energy introduced, whether through mechanical stimuli or acoustical vibrations, drives a liquid to transit on a solid between metastable states, overcome the energetic barriers, and reach the most stable wetting state, or one of the metastable states that are near to the most stable state. The study demonstrated that most stable or metastable contact angles can be measured for almost any imperfect solid. Such measurements are still not very popular because conventional instruments require considerable modification to accommodate speakers or other vibration-inducing devices [33, 67].

Importantly, the studies of contact angles during imposed vibrations confirmed that both advancing and receding contact angles relax to one value, the most stable contact angle. The work by Meiron et al. [34] additionally provided an experimental validation for the Wenzel equation. These authors also suggested, probably for the first time, that the droplet base tends to transition from an irregular to circular shape and that this symmetry is likely associated with the most stable state. This important observation was explored in our laboratory in detail [35] and will be discussed later using experimental data from adhesion force measurements.

It needs to be mentioned that the idea of adding vibrations to a liquid and/or solid sample during contact angle measurements is in fact much older than commonly recognized and has some roots in the 19th century. For example, Ablett used a rotating cylinder coated with paraffin wax to measure contact angles for water at varying rotation speeds and direction [68]. In his paper he pointed to a practice that was often executed during contact angle measurements in the past: "*…many writers insist on the necessity for tapping the capillary, or the plate on which drop rests, before taking readings but give no reason beyond that it pays to do so*." Unfortunately, Ablett did not provide any contact angle values before and after tapping. This approach of tapping the sample had quite deep roots in early research and received broad support among researchers at that and later times. For example, Wark wrote in 1938: "*…to ensure that a true equilibrium angle is obtained, the stage upon which the cell rests should be tapped lightly several times*"[69]. For some reason, this beneficial practice was surprisingly ignored and not explored for nearly 100 years.

Research on contact angle measurements carried out for solid specimens under vibrations is, however, not without faults. First, there is no means to confirm that vibrations culminate into liquid spreading at its most stable state. The microbalance approach presented in the second half of this contribution does not have this uncertainty. Second, the early reports promoted the following cosine correlation between equilibrium, advancing and receding contact angles, originally proposed by Adam and Jessop [70]:

$$cos\theta = \frac{cos\theta_A + cos\theta_R}{2} \qquad (6)$$

It will be shown later that the most stable contact angles cannot be predicted, or even, estimated, using equation (6).

Importance of Contact Line

Validity of the Wenzel, Cassie, and Cassie-Baxter equations has been questioned in many publications, as discussed in more detail in the previous review [16]. Raised concerns relate to parameters of these equations that describe sample surface heterogeneity and roughness, and whether these parameters should refer to surface characteristics as analyzed globally or only in the vicinity of contact line or at the contact line [71]. It is not always well appreciated that the thermodynamic relationships of Wenzel, Cassie and Cassie-Baxter are only valid when derived based on infinitely small displacements made by a liquid, over an area that does not change topography and/or heterogeneity pattern. Additionally, the size of a liquid drop, or contact line in general, must be orders of magnitude larger than any heterogeneity or asperity. For real surfaces such surface characteristics are rarely met and therefore surface landscape under the three-phase contact line and resulting shape of liquid perimeter are more important [40]. "Wetting contact line" does not fit to a mathematical one-dimensional definition of length. In the real world, surfaces and interfaces, and so the contact line, have vertical dimensions controlled by sizes of molecules and atoms. Additionally, a junction of three interfaces at the contact line experiences interfacial forces that contribute to its shape and characteristics [7]. Conceptually, therefore, there should be no difference in analysis of the surface landscape at contact line or in its close vicinity with appropriate understanding of contact line region and its range [40, 43, 72]. It is, however, more convenient to

just use the term of contact line, without going into details at molecular and nanoscopic levels that are still poorly understood. Overall, both Cassie and Cassie-Baxter equations require accommodation of contact line fractions instead of local area fractions.

Although a world-wide debate on the importance of contact line in analysis of contact angles on heterogeneous and rough surfaces was primarily triggered by the publication of Gao and McCarthy [73], this concept was around, but not appreciated, for quite some time. As early as 1945, Pease emphasized that it is the contact line and not contact area that needs to be taken into account in analysis of the work of adhesion for a liquid on a heterogeneous surface. Then, Swain and Lipowsky [74] replaced areal fraction with the fraction of droplet perimeter in the Cassie equation, a modification that was later validated through experimentation by Cubaud and Ferminger [75] and Larsen and Taboryski [76].

Microbalance – Camera System and its Advantages

Contact angles are often measured to access indirectly either adhesion or solid surface energy, both important quantities in formulation of coatings, painting, printing, de-icing, etc. The correlations between the advancing and receding contact angles and solid-liquid adhesion for solids with imperfect surfaces (having a certain degree of roughness and/or heterogeneity) are not straightforward, as indicated in previous sections, and at present are poorly understood. Experimental advancing and receding contact angles represent a combination of the effects associated with not only the solid surface energy but also sample geometry, size, and characteristics of roughness and heterogeneity. For this reason, some recent attempts have concentrated on direct measurements of liquid-solid interactions, initiated by the design of two apparatuses. The centrifugal adhesion balance, introduced in 2009, uses centrifugal and gravitational forces to induce different normal and lateral force combinations for direct adhesion measurements between a liquid drop and a solid surface [46, 77]. At about the same time, a microbalance was introduced by DataPhysics in Germany, which is presented in Figure 5.

With a specially designed hydrophobic loop to hold a water drop this balance is capable of measuring the liquid – solid surface interactions on drop-surface approach (spreading force) and pull-off force (adhesion) during water drop detachment. This instrument is a sensitive microbalance similar to what is typically used in Wilhelmy – type tensiometers. It allows the adhesion between a liquid drop and a solid of practically any shape and surface characteristics to be measured. It can also be used for force measurements in other systems involving either other liquids or gas bubbles. The profile of the interactions with respect to surface position (and time) is recorded automatically by the software. Concurrently, a CCD camera is used for recording of attachment, spreading, adhesion, and detachment events. The individual CCD frames are used to analyze the droplet shape and dimensions and to measure the contact angle at various stages of water droplet spreading and retreat (Figure 5).

Figure 6 shows an example of force curve for a water droplet in contact with polydimethylsiloxane (PDMS). The measurement starts with water droplet approaching polymer surface (force =0). When droplet touches the polymer surface at point A, contact is established and the water droplet spreads spontaneously until point B. The value of force measured at point B corresponds to spreading force [78]. At this point, the contact angle that is measured corresponds to advancing contact angle, and in most of the measurements this angle is of similar value as an advancing contact angle measured with a goniometer [78]. Between point B and C, the droplet is pushed against the solid to mechanically increase area of contact. This step can be avoided, especially if spread in liquid-solid contact area is not necessary. From point C, retraction takes place and droplet is stretched. Maximum force measured during stretching is at point D and is referred to as

maximum adhesion force, which corresponds to the most stable state in this measurement. Further stretching of the attached droplet reduces the liquid-solid contact area until point E, when pull-off force exceeds the adhesion force and droplet is either detached from the solid or broken into smaller drops, one remaining in the holding ring, and one attached the solid surface.

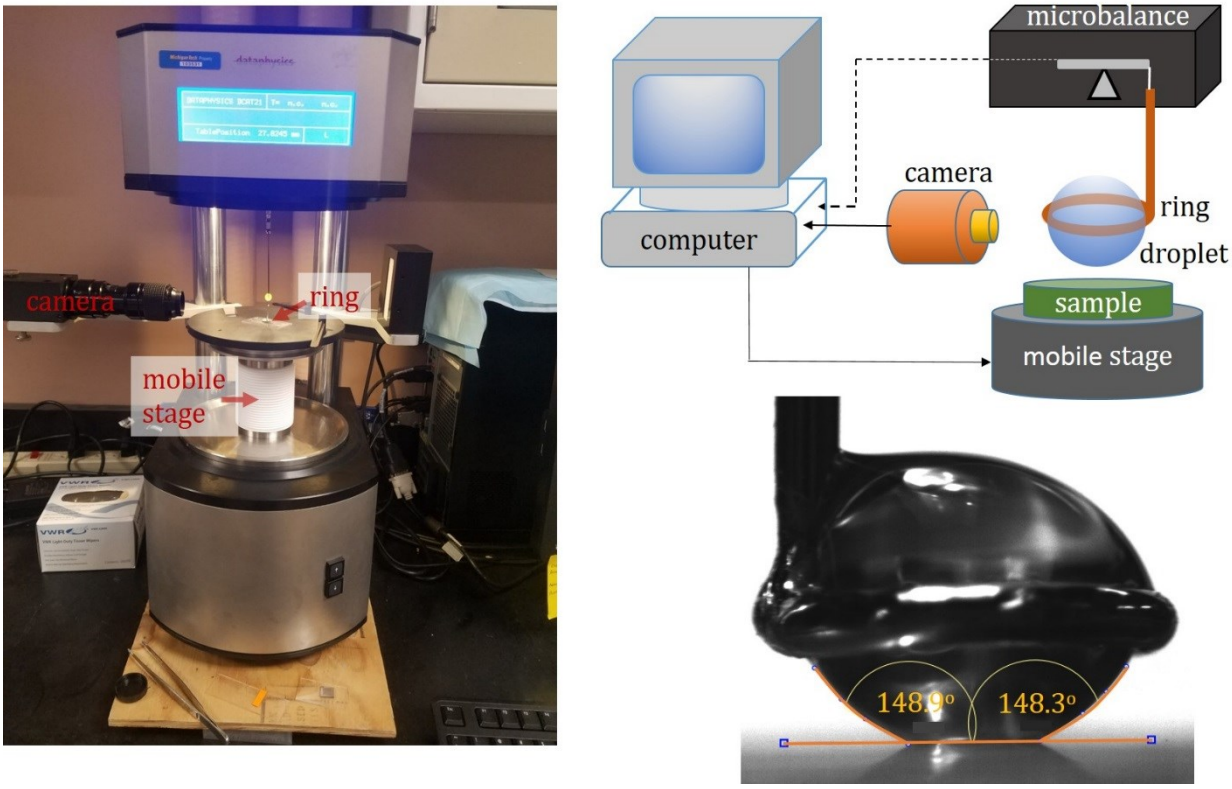

Figure 5. Microbalance and experimental set-up used in adhesion force measurements between water droplets and solids. Optical image of water droplet in contact with hydrophobic pattern with marked measured contact angles.

In summary, the system captures forces during spreading, adhesion at the most stable state, and during detachment. As a result, force barriers in transitions from spontaneous spreading to maximum adhesion and then pull-off can be quantified as well. Since contact angles are measured from captured images, they can be used for analysis of advancing, receding, and most stable contact angles and contact angle hysteresis. Measurements of contact angles for droplets in their most stable configuration using a microbalance is a significant advantage over the past attempts in which mechanical or acoustic vibrations were applied in an effort to reinforce a liquid to relax to the most stable state or near it. Using the microbalance – camera system simultaneously allows the contact angle at the exact point of most stable state to be determined.

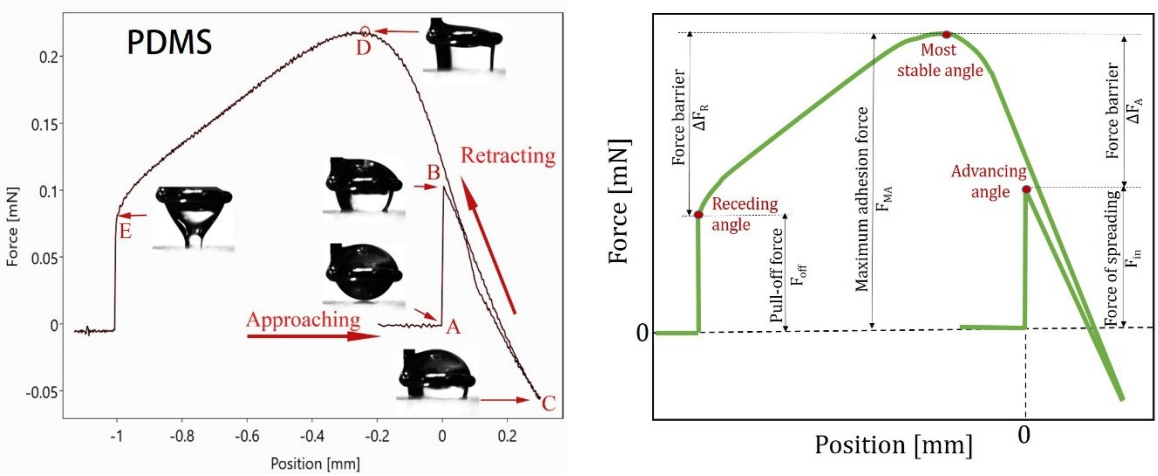

Figure 6. Force curve generated for PDMS sample (left) and its replica (right) with marked key parameters quantified from this curve. Insert images: images of water droplet at selected points of adhesion force measurements. The experimental force curve was reproduced from Ref. [78] with permission.

Adhesion Force Measurement Results

The following subsections describe the important outcomes from research conducted in our laboratories in the last two years, using the microbalance described above. Some of the results presented were already published [35, 78, 79], but new data are also included ahead of upcoming publications.

Most Stable versus Advancing and Receding Contact Angles

As discussed earlier, the current understanding is that an advancing contact angle measured on substrates of enhanced surface quality represent wetting characteristic of a solid surface and can be used in analysis of surface energy of polymers and other low-energy materials [62]. This hypothesis was recently challenged in our research [78] as described below. Table 1 summarizes the most stable contact angles measured for water droplets on four polymers of different surface chemistry and roughness, together with apparent advancing and receding contact angles determined through goniometry.

The most stable contact angles reported in Table 1 are of intermediate values from between apparent advancing and receding contact angles. Dozens of additional measurements carried out for PDMS patterns in our laboratory (not reported here) support these intermediate values, which are typically significantly lower than advancing contact angles and much closer to receding contact angles. This significant departure from advancing contact angle values is in contradiction with past statements, although in agreement with recent observations made by Martinelli et al.[50]. However, it remains unclear why advancing contact angles are significantly larger and receding contact angles much closer to most stable contact angles. One of the possibilities relates to disjoining pressure differences for precursor films surrounding the droplet in advancing and receding states. For example, Kuchin and Starov [51] concluded from theoretical modeling of disjoining pressure isotherms for liquid on smooth and homogeneous surfaces that the receding contact angle is much closer to the most stable contact angle (called equilibrium contact angle in this reference) than advancing contact angle, in contradiction with the view of advancing contact angles imposed in the 20th century literature.

Table 1. Experimental and calculated contact angles for four polymers (PDMS – polydimethyl silicone, EVA – ethylene vinyl acetate, PET – polyethylene terephthalate, Nylon – polyamide 6,6). RMS is the root mean square roughness as determined by atomic force microscopy. The contact angles include advancing (θ_A) and receding (θ_R) contact angles measured by goniometry, and most stable contact angle (θ_{max}) measured at maximum adhesion during force measurements. Data taken from Ref. [78]. Calculated contact angles are averaged values as per equations (6) and (8).

Sample	**RMS Roughness** [nm]	**By Goniometer**		**Average Calculated**		**By Microbalance**
		θ_A [deg]	θ_R [deg]	By Eq. (8) [deg]	By Eq.(6) [deg]	θ_{max} (most stable) [deg]
PDMS	6 ± 4	117 ± 2	78 ± 1	98	97	91 ± 3
EVA	340 ± 200	100 ± 2	77 ± 2	89	89	77 ± 3
PET	4 ± 1	77 ± 1	54 ± 1	66	66	57 ± 3
Nylon	11 ± 6	63 ± 1	29 ± 1	46	48	37 ± 3

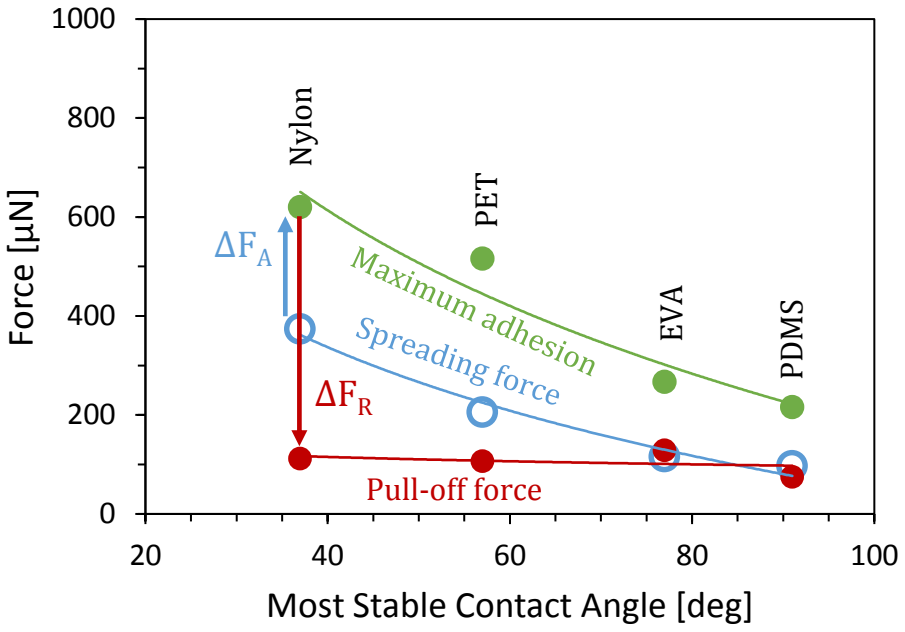

Figure 7. Mean values of spreading, maximum adhesion and pull-off forces measured for water droplets in contact with PDMS, EVA, PET and Nylon samples (see Table 1 for advancing, receding and most stable contact angles for water droplets on these polymers). Force barriers between most stable state and two other states: spontaneous spreading state and most receding state are marked with arrows and ΔF_A and ΔF_R, respectively. The numerical values for force barriers are listed in Table 2.

Interpretation of both advancing and receding contact angles requires, therefore, further investigation. Here, force barriers between advancing, most stable, and receding states are analyzed. Figure 7 shows correlations between spreading force, maximum adhesion force and pull-off force and most stable contact angle for the four polymers under discussion. Three of these polymers had roughness at a level of a few nanometers and only EVA had roughness nearly two orders of magnitude larger (Table 1). As a result, adhesion force data for EVA (discussed later) were typically less consistent than for other polymers but mean force values followed the force vs. contact angle trendlines for other polymers (Figure 7).

The force measurements confirmed increasing adhesion forces with increasing affinity of polymers to water reflected by decrease in the most stable contact angle (Figure 7). At first glance, there appears to be very little effect of roughness on forces and their correlations; surface nanoroughness alone cannot explain correlations presented in Figure 7. For all four polymers, the spreading force had a lower value than maximum adhesion force, and the force barriers, ΔF_A (calculated as the difference between maximum and spreading forces) and ΔF_R (the difference between maximum and pull-off forces) (Table 2), increased for polymers with increasing hydrophilicity. It is concluded, therefore, that surface chemistry of polymer and its adhesion with water are likely additional causes for correlations in Figure 7.

Since the droplet base differed at each stage of adhesion force measurements, the force barriers can be normalized per unit length of contact line. In this study, the measured force was normalized using the following equation:

$$dF_{ij} = \left| d\left(\frac{F}{l}\right)_{ij} \right| \tag{7}$$

Therefore, a force barrier between spontaneous spreading and most stable states is:

$$\Delta F_A = \left| \left(\frac{F_{in}}{2\pi R_{in}} - \frac{F_{max}}{2\pi R_{max}} \right) \right| \tag{7a}$$

and force barrier between most stable and pull-off states is:

$$\Delta F_R = \left| \left(\frac{F_{max}}{2\pi R_{max}} - \frac{F_{off}}{2\pi R_{off}} \right) \right| \tag{7b}$$

As shown in Table 2, the normalized force barriers follow a similar trend as in Figure 7 and increase with increasing hydrophilicity of polymers (expressed by contact angle).

Table 2. The force barriers between spontaneous spreading and most stable state (ΔF_A), and most receding and most stable states (ΔF_R), presented as raw data from Figure 7 and normalized per unit length of contact line as per equation (7). (*Uncertainty was calculated using error propagation analysis; **Only mean values are presented.)

Sample	**Most Stable Contact Angle [deg]**	**Force Barrier**					
		Raw Data* [μN]			**Normalized** [mN/m]**		
		ΔF_A	**ΔF_R**	**Total**	**ΔF_A**	**ΔF_R**	**Total**
PDMS	91 ± 3	119 ± 3	141 ± 3	260 ± 4	17	7	24
EVA	77 ± 3	151 ± 24	138 ± 22	289 ± 33	34	6	40
PET	57 ± 3	310 ± 19	409 ± 12	719 ± 22	40	45	85
Nylon	37 ± 3	246 ± 13	508 ± 10	754 ± 16	22	59	81

A fundamental question is whether a liquid could spread spontaneously to the most stable state on a perfectly smooth surface. Preparation of solid specimens that have atomically smooth and homogeneous surfaces is extremely difficult and quite often impractical. Even carefully prepared polymeric films used in our research have roughness at a level of at least a few nanometers. There is no guarantee that this "residual" roughness can be ignored in measurements of advancing and receding contact angles when following a common contact angle measurements practice such as in Ref. [25]. For this reason, attention was switched to liquids with surfaces that are smooth and their surface homogeneity can be controlled by purity of liquid and elimination of any possibility of surface adsorption of contaminants from the air. Our preliminary experiments involved saturated hydrocarbons as per list in Table 3. Before experimental data are discussed, however, it should be mentioned that liquid spreading in these experiments is different than for water droplets in contact with solids. Instead of droplet spreading, hydrocarbons climb over the water droplet surface, as per image insert of Figure 8 that shows hexadecane meniscus surrounding a water droplet.

An example of one of the force curves recorded for a water droplet in contact with hexadecane is shown in Figure 8. The force curves for liquid-liquid systems appear similar to those recorded for liquid-solid systems, showing similar shapes with characteristic transition points representing spreading, maximum adhesion and pull-off forces. Table 3 summarizes mean force values and their standard deviations for three hydrocarbons used in our study. This table also shows similar data for a non-polar solid, PDMS, since its surface energy is somewhat close to surface energy of saturated hydrocarbons.

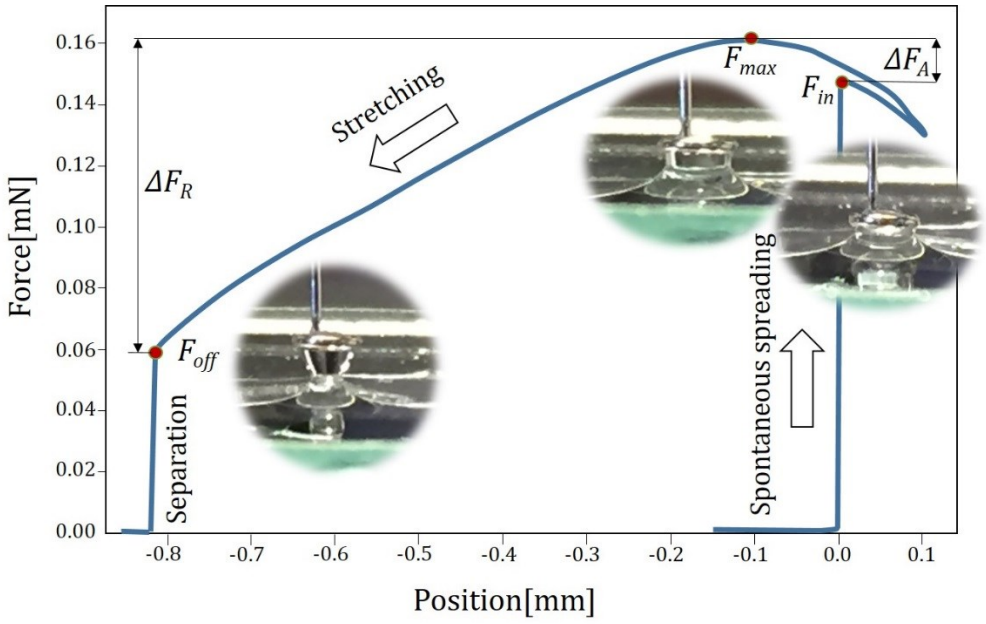

Figure 8. The force curve for water droplet in contact with hexadecane. The graph is a replica of the result after the curve was smoothed to eliminate fluctuation of line caused by vibrations during measurements. The inserts show photographs taken during adhesive contact of water droplet with hexadecane at points of spreading force, maximum adhesion and pull-off force. Symbols include: F_{in} – spreading force, F_{max} – maximum adhesion force, F_{off} – pull off force, ΔF_A – force barrier between spreading force and maximum adhesion force, and ΔF_R – force barrier between pull off force and maximum adhesion force.

The measurements with hydrocarbons revealed the following key findings, shedding important light on spreading of liquid droplets on solids. First, spontaneous spreading of hydrocarbons on water droplets never reached the most stable state. This suggests, as expected but never proven, that spontaneous spreading is under non-equilibrium conditions, even in its final stages, and during the typical timeframe of experimental observations. In the case of hydrocarbon spreading over the water droplet, the most likely cause of a barrier between F_{in} and F_{max} is related to structure of a precursor film that spreads ahead of bulk liquid and a delay in saturation of both contacted liquids with each other. Selected test with saturated liquids (not shown) performed in our study suggests that the second factor is rather less important, but this spreading process still requires more detailed investigation. In support of this finding it should be mentioned that contact angle hysteresis has already been reported on free liquid films in the past, which are also smooth, chemically homogenous and deformable [80, 81]. In addition, theoretical calculations of disjoining pressure isotherms for a liquid drop on smooth and homogeneous surfaces clearly suggest the presence of contact angle hysteresis that results from different thickness of a precursor film for liquid advancing and retreating [51]. Although the theoretical analysis was done for solid surfaces, general conclusions should apply to the current liquid/liquid situation.

Table 3. Means and standard deviations of forces measured for water drops in contact with hydrocarbons. (*Uncertainty was calculated using error propagation analysis.)

Hydrocarbon	**Force [μN]**			**Force Barrier* [μN]**	
	$\mathbf{F_{in}}$	$\mathbf{F_{max}}$	$\mathbf{F_{off}}$	$\mathbf{\Delta F_A}$	$\mathbf{\Delta F_R}$
Hexadecane	138 ± 6	163 ± 3	62 ± 4	25 ± 7	101 ± 5
Decane	180 ± 20	207 ± 1	81 ± 1	27 ± 20	126 ± 1
Nonane	160 ± 20	200 ± 2	74 ± 5	40 ± 20	126 ± 5
Comparison to solid:					
PDMS	97 ± 1	216 ± 3	75 ± 1	119 ± 2	141 ± 2

Additionally, the difference between F_{in} and F_{max} was found to be 3-7 times smaller for a liquid-liquid system than for systems with solids. This suggests that solid surface imperfections, even as small as several nanometers in dimensions, are likely influencing spontaneous spreading (and the resulting advancing contact angle).

A significant difference between force at most stable state (F_{max}) and that measured during separation (F_{off}) was recorded in all measurements. As shown in Table 3, the value of ΔF_R is close to what was measured for PDMS. This further confirms that this barrier is mainly related to interfacial interactions (adhesion), and surface imperfections appear to be less important, at least for polymers which had a nearly smooth and homogeneous surface.

In summary, in view of our findings for both liquid-solid and liquid-liquid systems, spontaneous spreading advances liquid over a substrate surface but culminates ahead of the most stable state. Therefore, it appears inappropriate to use the advancing contact angle as an indicator of intrinsic property of substrate including surface energy, chemistry or hydrophilicity/hydrophobicity. Most stable contact angles should be used for this purpose instead, or at least complement current ranking of materials based on advancing contact angles. Further, the use of most stable contact angles will likely require adjustments in semi-empirical models developed for solid surface energy

calculations from experimental contact angles. This conclusion is in line with recommendations made by others [50].

Testing Averaged Contact Angles

A difference between advancing and receding contact angles was already noticed at the beginning of the 20th century. Since that time, many attempts have concentrated on calculations of average contact angles, in an effort to estimate most stable contact angles such as those represented by the Young's, Wenzel, Cassie and Cassie-Baxter equations. For example, Ablett used the method of a rotating cylinder coated with paraffin wax to measure contact angles for water at varying rotational speeds and direction, and then calculated mean contact angle as per simple arithmetic formula [68]:

$$\theta = \frac{\theta_A + \theta_R}{2} \qquad (8)$$

He believed that the calculated values represent characteristic values for the surfaces examined.

It was Adam and Jessop who proposed a cosine function for calculations of equilibrium contact angles, expressed by equation (6) as presented earlier [70]. As already discussed, equation(6) is sometimes used, since two decades ago, to calculate average values, which are supposed to be close to most stable contact angles.

Table 1 shows data from our own research with the microbalance. It is clear that averaged advancing and receding contact angles, whether calculated based on arithmetic average (8) or cosine function (6), do not match most stable contact angles determined experimentally with microbalance. These discrepancies align with results presented in earlier reports [34, 50] when measurements of most stable contact angles took place after acoustic vibrations.

It needs to be emphasized that when θ_A and θ_R are not too different, the cosine of the angle calculated from equation (6) is quite close to that calculated from equation (8). Thus, it does not make much difference which of them is used. Overall, neither equation (6) nor (8) should be used in calculation of most stable contact angle.

In recent years, several attempts were made to predict most stable contact angles (referred usually to as equilibrium or Young contact angles in these references) based on advancing and receding contact angle values [82-84]. Analysis of these new models, however, is beyond the scope of this review and will be addressed in future publications.

Testing Symmetry of Droplets

Three anisotropic rough patterns, made of parallel 5 μm – wide PDMS ridges spaced by 5 to 20 μm – wide grooves (the solid fraction φ was 0.50, 0.33 and 0.20, respectively), were used in our study (named as groove55, groove510 and groove520 in Figure 9) to study contact angles at different stages of spreading and separation along longitudinal and traverse directions [35]. The study confirmed that water droplets spread anisotropically, and favor an anisotropic base over an asymmetric one during spontaneous spreading on above-mentioned samples, expanding their dimensions by up to 70% along the longitudinal direction as compared to the traverse direction [35]. Contact angles measured in a traverse direction to the pattern during spontaneous spreading varied among the patterns no more than 4 degrees, despite the different groove spacing of the three patterns. These results confirmed that the geometrical dimensions and shape of structured patterns made of hydrophobic material do not have strong influence on contact angles during spontaneous spreading over a dry pattern [85].

The contact angle values measured in the traverse direction were higher than those measured in the longitudinal direction. These differences decreased from about 20 degrees for the groove pattern with 5 μm spacing to less than 10 degrees for the groove pattern with 20 μm spacing, showing larger anisotropy in the droplet shape for a pattern with smaller spacing between ridges and greater value of solid fraction (Figure 9). These differences, however, vanished at the point of maximum adhesion force (Figure 9). The merger of contact angle values coincided with the alteration of the axisymmetric ellipsoid droplet base to a circle one with a base diameter ratio between longitudinal and traverse dimensions equal to 1 [35]. This conversion to the circular base happened for all three samples at a maximum adhesion force value and provides additional support for our interpretation that the point of maximum adhesion force is affiliated with the most stable state.

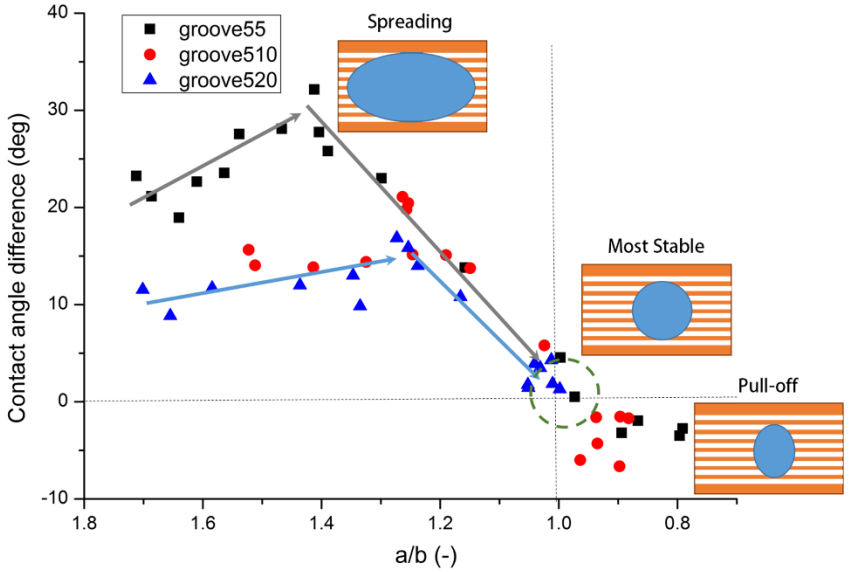

Figure 9. Difference in contact angle measured along transverse and longitudinal directions as a function of aspect ratio for droplet diameters at different stages of droplet spreading, compression, stretching and separation. Reproduced from Ref. [35] with permission.

Our experiments prove that the water droplet prefers its symmetrical base, even for a very anisotropic pattern, which corresponds to the most stable configuration (having a minimum energy). This phenomenon is not limited to the anisotropic patterns used in this study, and similar observations were made for pillar- and pore-structured PDMS patterns (not shown). Therefore, the droplet shape evolves to become axisymmetric at the most stable state regardless of the surface roughness, as long as the droplet is large enough compared to roughness feature dimensions and there is enough driving energy to overcome the energy barriers. It appears, therefore, that *the base of droplet is circular at the most stable state because the circle has the shortest perimeter per surface area and therefore the droplet is in its lowest energetic state*. This is similar to a sphere where surface area is minimized per unit volume for this shape.

Testing Validity of Theoretical Models

As discussed earlier, the Wenzel, Cassie and Cassie-Baxter equations pertain only to the most stable states. Analysis of both the Wenzel and Cassie equations cannot be provided yet due to a

limited selection of solid samples examined in our study. Because our studies only included patterns made of hydrophobic PDMS, the discussion is restrained to the Cassie-Baxter equation.

Going back to experimental data for anisotropic patterns discussed in a previous sub-section, and using the areal solid fractions and a contact angle of ~91 degree for PDMS at most stable state of water droplets (Table 4) [78], the Cassie-Baxter equation predicts that the contact angles should be equal to 120, 132, and 143° for parallel grooves: 5x5, 5x10, and 5x20 μm, respectively. These values are nearly identical to experimental contact angle values measured at the most stable states along longitudinal and traverse directions of grooved patterns, as shown in Table 4. This agreement is attributed to the very symmetrical structure of patterns used, where areal solid fractions are nearly identical to linear fractions.

Table 4. Summary of contact angles measured from two directions at MAF and calculated Cassie-Baxter contact angles using areal solid fractions [35].

Pattern	**Experimental Contact Angles** [deg]		**Prediction from Cassie-Baxter** [deg]
	$\theta_{//}$	$\theta_{\perp}$	
5x5 μm (f_S = 0.50)	119 ± 2	118 ± 2	120
5x10 μm (f_S = 0.33)	130 ± 2	128 ± 2	132
5x20 μm (f_S = 0.20)	138 ± 2	142 ± 2	143

Our most recent studies (conducted in collaboration with the Stevens Institute of Technology and involving more complex hydrophobic patterns) revealed a weakness of the Cassie-Baxter model when areal solid fraction is used in analysis of most stable contact angles. The patterns recently fabricated included perforated PDMS with square-shaped pores as well as PDMS pillars having circular and square cross sections. Dimensions of pores and pillars varied from 2.5 to 50 microns. All patterns and adhesion force values measured will be presented in detail in a separate publication.

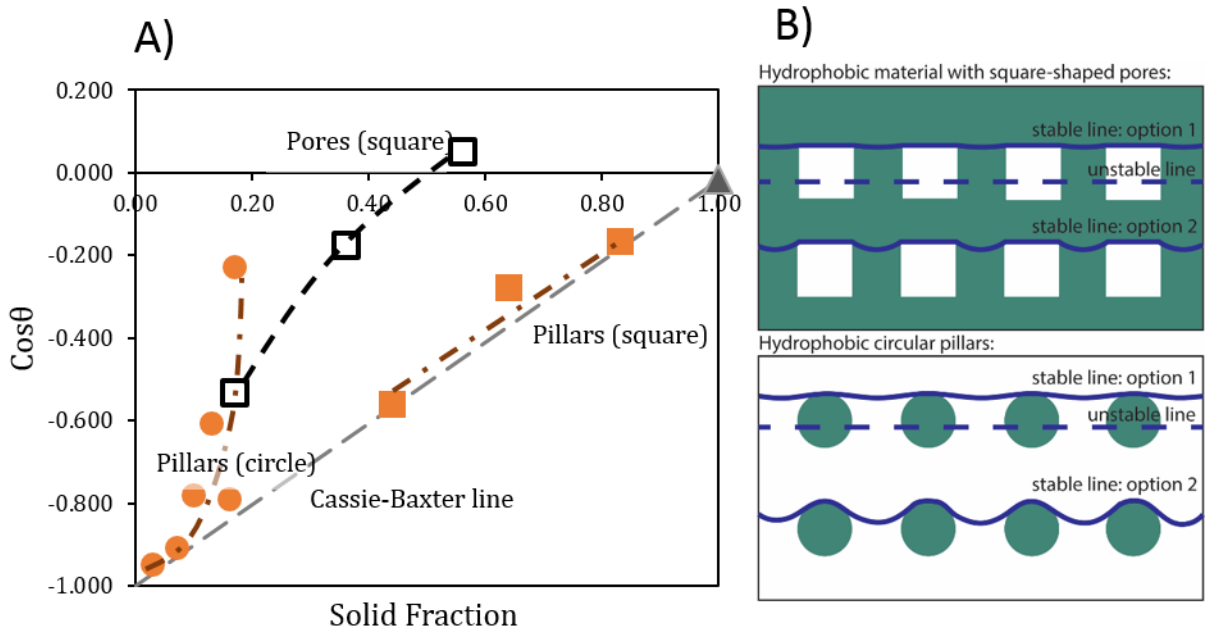

Figure 10. A) Cosine of most stable contact angles (cosθ) versus areal solid fraction of PDMS pattern. Results are for water droplets in contact with PDMS patterns made of pillars (both circular and square cross-section) and PDMS perforated with square shaped pores. Details of patterns will be presented separately. B) Schematics of water droplet contact line on perforated hydrophobic material with square-shaped pores (top) and on circular-cross section pillars made of hydrophobic material (bottom). Position 1 and 2 describe contact line in advanced and receded movement, and broken line represents contact line in unstable position.

The most stable contact angles are plotted as a cosine function versus solid fraction in Figure 10A. As shown, the correlation deviates significantly from the Cassie-Baxter equation for most of the patterns. Only samples with square pillars or circular pillars of small density follow the Cassie-Baxter prediction. This finding is in agreement with the work of Choi et al. [86] who demonstrated that differential areal fraction of a solid pattern covered by the three-phase contact line is the most important factor in shaping the liquid with advancing and receding contact angles.

All points above the line representing the Cassie-Baxter equation in Figure 10A indicate a larger contribution of solid for the contact line than areal analysis suggests. This is indicative of water favoring contact with a hydrophobic solid at the expense of contact with air-filled spacing. As shown with schematics in Figure 10B, the contact line attempts to maximize its presence at solid surface through escaping the air pockets that often can lead to significant contortion of the contact line. In support of this statement, examples of contact line visualization on PDMS patterns using inverted optical microscopy were provided in our previous contribution [78]. More detailed analysis of contact line for patterns discussed in relation to Figure 10 will be provided in a separate publication.

Conclusions

Modern interpretation of advancing and receding contact angles, and contact angle hysteresis, and their use in classification of solids and determination of solid surface energy (and its parameters) require refinement and new approaches. Our recent force measurements for water droplets in contact with solids and liquids and concurrent measurements of contact angles led us to the following conclusions:

- Using a microbalance equipped with a CCD camera allows the capturing of changes in shape of droplets during attachment and spreading, droplet compression and detachment, and quantify forces of spreading, adhesion and detachment. The instrument is also suitable to measure the adhesion forces in liquid-liquid systems.
- Droplet spreading over the solid surface is driven by spreading force that directly correlates with advancing contact angle [79]. The spreading force is always smaller than force of maximum adhesion that represents the droplet at most stable interfacial contact with solid or liquid. The difference between spreading force and maximum adhesion force is affected by solid surface imperfections but was also recorded for perfectly smooth surface of liquids. This experimental finding suggests a contribution of other factors than roughness and heterogeneity to contact angle hysteresis.
- Maximum adhesion and then pull-off forces required for separation of water droplet from substrate are in direct correlation with the contact angles that are closer to apparent receding contact angles than apparent advancing contact angles for solid surfaces having either different wetting characteristic or topography or both.
- Interfacial interactions for liquids in contact with solids contribute to contact angle hysteresis. In other words, the assumption that the contact angle hysteresis is absent for ideal surfaces is likely incorrect and should be challenged.
- The most stable configuration for a liquid droplet on a solid surface appears only when the droplet base is axisymmetric. A contortion of the contact line is still possible at this state because the droplet attempts to establish the strongest adhesion through an increase in contact with surface component of higher affinity to liquid.
- Limited research with patterned surfaces suggests that the location and quantification of length and shape of the three-phase contact line are needed (see also Refs [78, 86, 87]) to verify models describing most stable contact angles such as the Wenzel, Cassie, and Cassie-Baxter models.
- Averaging of cosines of advancing and receding contact angles can lead to contact angle values that are significantly different than contact angles measured experimentally at the most stable state. See also Refs [34, 50].

Upcoming Challenges

There are some important challenges that can be suggested from the recent research conducted in our laboratory:

- Contact angles measured at point of maximum adhesion force, which represent the most stable state under experimental conditions, could be used in characterization of solid surfaces. This opens a new prospect for classification of solids and liquids regarding their affinity to water and other liquids.

- The instrument allows measurement of the values of force barriers between metastable states during liquid droplet spreading and retreat but this course was not explored in our program yet due to force barriers that are typically comparable in value to the noise level in force measurements for patterns tested in our current research.
- Cause of the difference between maximum adhesion and pull-off force is not fully understood. Both liquid-solid and liquid-liquid systems show such a difference and both should be studied in details to understand roots of hysteresis that have origins in interactions at interfaces/contact lines.
- Location and shape of the three-phase contact line during adhesion force measurements cannot be recorded in current microbalance-camera set-up and additional improvement is needed in order to correlate experimental force values with characteristics of the three-phase contact line.

Comment on the Most Critically Important Finding

Contact angle hysteresis on smooth and homogeneous surfaces is driven by forces of interfacial interactions. It should receive more attention than other effects such as roughness, heterogeneity, etc. in the immediate future. Systems that are free of hysteresis do not exist in our world. If there would not be hysteresis, the slightest external stimuli would initiate movement of the contact line on "ideal" surfaces, which could result in:

1) Tendency of a liquid to reach most stable state, regardless of droplet deposition method, in a very short time and for very short duration;
2) Tendency of a liquid to remain in unstable states, resulting with ever-changing shape of droplet; and
3) This would also result in impossibility of executing phase aggregation and phase separation processes, which are important to many industrial operations.

It would be only possible for interfaces with no interatomic/intermolecular interactions, which obviously is not possible. Sulman [56] was probably the first scientist who considered the significance of contact angle hysteresis in separation of matter. He referred to flotation of particles and speculated that a particle-bubble aggregate could be unstable if it relied on one "equilibrium" contact angle; any departure from stable state could sink the mineral particle. He stated that the contact angle hysteresis *permits a wider range of equilibrium for a floating particle*. Surprisingly he did not have any clear explanation of contact angle hysteresis and wrote: "*…the hysteresis 'drag' appears to be caused by some sort of molecular interlocking between the solid and liquid surfaces*."

Acknowledgments

This paper is the result of the encouragement and trust of Professors Boinovich and Emelyanenko of the Russian Academy of Sciences. I would like to express my sincere appreciation to both of them and the other organizers of the 16th International Conference on Surface Forces for the opportunity to present my keynote address and visit the beautiful Russian city of Kazan. I also appreciate valuable comments from Prof. Ludmila Boinovich received during manuscript review process.

Most of the experiments done with solid samples briefly reviewed in this paper are the result of a fruitful collaboration with Prof. Chang-Hwan Choi and Youhua Jiang (already graduated with a PhD degree) from the Stevens Institute of Technology (SIT). Specimens of PDMS and its various patterns were prepared at SIT and force measurements were carried out at Michigan Tech by a scholar Yujin Sun (graduated with a PhD degree at China University of Mining and Technology). All

measurements of spreading and adhesion forces for liquid-liquid systems presented in this contribution were carried out by Benjamin Gregory. The author would also like to express appreciation to Dr. Helen Rau for drawing schematics for this review (Figures 1, 2, and 10). Editing corrections from Adam J Drelich are appreciated by the author.

Financial support for purchasing atomic force microscope used in characterization of polymer roughness through NSF-CS-MRI grant (#1725818) is appreciated as well.

References

[1] Marmur A, Della Volpe C, Siboni S, Amirfazli A, Drelich JW. Contact angles and wettability: towards common and accurate terminology. Surface Innovations. 2017;5:3-8.
[2] Young T. An essay on the cohesion of fluids. Philosophical Transactions of the Royal Society of London. 1805;95:65-87.
[3] Wenzel RN. Resistance of solid surfaces to wetting by water. Ind Eng Chem. 1936;28:988-94.
[4] Cassie ABD. Contact angles. Discussions of the Faraday Society. 1948;3:11-6.
[5] Cassie ABD, Baxter S. Wettability of porous surfaces. Trans Faraday Soc. 1944;40:546-51.
[6] Whyman G, Bormashenko E, Stein T. The rigorous derivation of Young, Cassie-Baxter and Wenzel equations and the analysis of the contact angle hysteresis phenomenon. Chem Phys Lett. 2008;450:355-9.
[7] Drelich J. The significance and magnitude of the line tension in three-phase (solid-liquid-fluid) systems. Colloid Surf A-Physicochem Eng Asp. 1996;116:43-54.
[8] Marmur A. Line tension and the intrinsic contact angle in solid-liquid-fluid systems. Journal of Colloid and Interface Science. 1997;186:462-6.
[9] Boinovich L, Emelyanenko A. Wetting and surface forces. Advances in Colloid and Interface Science. 2011;165:60-9.
[10] Marmur A. Wetting on hydrophobic rough surfaces: To be heterogeneous or not to be? Langmuir. 2003;19:8343-8.
[11] Wolansky G, Marmur A. Apparent contact angles on rough surfaces: the Wenzel equation revisited. Colloid Surf A-Physicochem Eng Asp. 1999;156:381-8.
[12] Brandon S, Haimovich N, Yeger E, Marmur A. Partial wetting of chemically patterned surfaces: The effect of drop size. Journal of Colloid and Interface Science. 2003;263:237-43.
[13] Marmur A. Solid-surface characterization by wetting. Ann Rev Mater Res. Vol. 39. Palo Alto: Annual Reviews; 2009. p. 473-89.
[14] Derjaguin BV. Theory of capillary condensation and other capillary phenomena accounting for the disjoining pressure of polymolecular liquid films. Acta Physicochimia URSS. 1940;12:181-200.
[15] Bangham DH, Razouk RI. Adsorption and the wettability of solid surfaces. Trans Faraday Soc. 1937;33:1459-63.
[16] Drelich J, Chibowski E, Meng DD, Terpilowski K. Hydrophilic and superhydrophilic surfaces and materials. Soft Matter. 2011;7:9804-28.
[17] Drelich J, Marmur A. Physics and applications of superhydrophobic and superhydrophilic surfaces and coatings. Surface Innovations. 2014;2:211-27.
[18] Boruvka L, Neumann AW. Generalization of classical theory of capillarity. J Chem Phys. 1977;66:5464-76.
[19] Wolansky G, Marmur A. The actual contact angle on a heterogeneous rough surface in three dimensions. Langmuir. 1998;14:5292-7.
[20] Eick JD, Good RJ, Neumann AW. Thermodynamics of contact angles. 2. Rough solid surfaces. Journal of Colloid and Interface Science. 1975;53:235-48.

[21] Neumann AW, Good RJ. Thermodynamics of contact angles. 1. Heterogeneous solid surfaces. Journal of Colloid and Interface Science. 1972;38:341-58.
[22] Schwartz LW, Garoff S. Contact-angle hysteresis on heterogeneous surfaces. Langmuir. 1985;1:219-30.
[23] Ruiz-Cabello FJM, Rodriguez-Valverde MA, Cabrerizo-Vilchez MA. Equilibrium contact angle or the most-stable contact angle? Advances in Colloid and Interface Science. 2014;206:320-7.
[24] Ruiz-Cabello FJM, Rodriguez-Valverde MA, Cabrerizo-Vilchez M. A new method for evaluating the most stable contact angle using tilting plate experiments. Soft Matter. 2011;7:10457-61.
[25] Drelich J. Guidelines to measurements of reproducible contact angles using a sessile-drop technique. Surface Innovations. 2013;1:248-54.
[26] Huhtamaki T, Tian XL, Korhonen JT, Ras RHA. Surface-wetting characterization using contact-angle measurements. Nat Protoc. 2018;13:1521-38.
[27] Marmur A. A guide to the equilibrium contact angles maze. In: Mittal KL, (editor). Contact Angle, Wettability and Adhesion. Vol. 6. Leiden: Koninklijke Brill NV; 2009. p. 3-18.
[28] Drelich J. Instability of the three-phase contact region and its effect on contact angle relaxation. J Adhes Sci Technol. 1999;13:1437-55.
[29] Boinovich L, Emelyanenko A. Characterizing the physicochemical processes at the interface through evolution of the axisymmetric droplet shape parameters. In: Mittal KL, (editor). Advances in Contact Angle, Wettablility and Adhesion. Vol. 3. Beverly, MA: Scrivener Publishing LLC; 2018. p. 99-129.
[30] Belman N, Jin KJ, Golan Y, Israelachvili JN, Pesika NS. Origin of the Contact Angle Hysteresis of Water on Chemisorbed and Physisorbed Self-Assembled Monolayers. Langmuir. 2012;28:14609-17.
[31] Chen SY, Kaufman Y, Schrader AM, Seo D, Lee DW, Page SH, et al. Contact angle and adhesion dynamics and hysteresis on molecularly smooth chemically homogeneous surfaces. Langmuir. 2017;33:10041-50.
[32] Decker EL, Garoff S. Using vibrational noise to probe energy barriers producing contact angle hysteresis. Langmuir. 1996;12:2100-10.
[33] Della Volpe C, Maniglio D, Morra M, Siboni S. The determination of a 'stable-equilibrium' contact angle on heterogeneous and rough surfaces. Colloid Surf A-Physicochem Eng Asp. 2002;206:47-67.
[34] Meiron TS, Marmur A, Saguy IS. Contact angle measurement on rough surfaces. Journal of Colloid and Interface Science. 2004;274:637-44.
[35] Sun YJ, Jiang YH, Choi CH, Xie GY, Liu QX, Drelich JW. The most stable state of a droplet on anisotropic patterns: support for a missing link. Surface Innovations. 2018;6:133-40.
[36] Drelich JW, Marmur A. Meaningful contact angles in flotation systems: critical analysis and recommendations. Surface Innovations. 2018;6:19-30.
[37] Chen YL, Helm CA, Israelachvili JN. Molecular mechanisms associated with adhesion and contact angle hysteresis of monolayer surfaces. Journal of Physical Chemistry. 1991;95:10736-47.
[38] Wang YJ, Guo S, Chen HY, Tong PE. Understanding contact angle hysteresis on an ambient solid surface. Phys Rev E. 2016;93:10.
[39] Dettre RH, Johnson RE, Jr. Contact angle hysteresis. IV. Contact angle measurements on heterogeneous surfaces. The Journal of Physical Chemistry. 1965;69:1507-15.
[40] Drelich J. Static contact angles for liquids at heterogeneous rigid solid surfaces. Pol J Chem. 1997;71:525-49.
[41] Dettre RH, Johnson RE, Jr. Contact angle hysteresis. II. Contact angle measurements on rough surfaces. In: Fowkes FM, (editor). Advances in Chemistry Series: Contact Angle, Wettability and Adhesion. Vol. 43. Washington, D.C.: American Chemical Society; 1964. p. 136-44.
[42] Extrand CW. Model for contact angles and hysteresis on rough and ultraphobic surfaces. Langmuir. 2002;18:7991-9.
[43] De Gennes PG. Wetting - statics and dynamics. Rev Mod Phys. 1985;57:827-63.

[44] Marchand A, Das S, Snoeijer JH, Andreotti B. Contact Angles on a Soft Solid: From Young's Law to Neumann's Law. Physical Review Letters. 2012;109:5.
[45] Shanahan MER. The influence of solid micro-deformation on contact angle equilibrium. J Phys D-Appl Phys. 1987;20:945-50.
[46] Tadmor R, Bahadur P, Leh A, N'Guessan HE, Jaini R, Dang L. Measurement of Lateral Adhesion Forces at the Interface between a Liquid Drop and a Substrate. Physical Review Letters. 2009;103:266101.
[47] Lester GR. Contact angles of liquids at deformable solid surfaces. Journal of Colloid Science. 1961;16:315-26.
[48] Leh A, N'Guessan HE, Fan JG, Bahadur P, Tadmor R, Zhao YP. On the Role of the Three-Phase Contact Line in Surface Deformation. Langmuir. 2012;28:5795-801.
[49] Tretinnikov ON, Ikada Y. Dynamic wetting and contact-angle hysteresis of polymer surfaces. Studies with the modified Wilhelmy balance method. Langmuir. 1994;10:1606-14.
[50] Martinelli E, Galli G, Cwikel D, Marmur A. Wettability and Surface Tension of Amphiphilic Polymer Films: Time-Dependent Measurements of the Most Stable Contact Angle. Macromol Chem Phys. 2012;213:1448-56.
[51] Kuchin I, Starov V. Hysteresis of Contact Angle of Sessile Droplets on Smooth Homogeneous Solid Substrates via Disjoining/Conjoining Pressure. Langmuir. 2015;31:5345-52.
[52] Derjaguin BV, Churaev NV, Muller VM. Surface Forces. New York and London: Consultant Bureau; 1987.
[53] Fisher LR. Measurement of small contact angles for sessile drops. Journal of Colloid and Interface Science. 1979;72:200-5.
[54] Schwartz AM. Contact angle hysteresis: a molecular interpretation. Journal of Colloid and Interface Science. 1980;75:404-8.
[55] Extrand CW, Kumagai Y. An experimental study of contact angle hysteresis. Journal of Colloid and Interface Science. 1997;191:378-83.
[56] Sulman HL. A contribution to the study of flotation. Transactions of the Institution of Mining and Metallurgy. 1919;29:44-138.
[57] Lord Rayleigh. On the tension of water surfaces, clean and contaminated, investigated by the method of ripples. Philosophical Magazine. 1890;5th Series (30):386-400.
[58] Johnson RE, Jr., Dettre RH. Contact angle hysteresis. I. Study of an idealized rough surface. In: Fowkes FM, (editor). Advances in Chemistry Series: Contact Angle, Wettability, and Adhesion. Vol. 43. Washington, D.C.: American Chemical Society; 1964. p. 112-35.
[59] Johnson RE, Jr., Dettre RH. Wettability and contact angles. In: Matijevic E, (editor). Surface and Colloid Science. Vol. 2. New York: Wiley-Interscience; 1969. p. 85-153.
[60] Johnson RE, Jr., Dettre RH. Contact angle hysteresis. III. Study of an idealized heterogenous surface. The Journal of Physical Chemistry. 1964;68:1744-50.
[61] Good RJ. Contact-angle, wetting, and adhesion - a critical-review. J Adhes Sci Technol. 1992;6:1269-302.
[62] David R, Neumann AW. Contact angle patterns on low-energy surfaces. Advances in Colloid and Interface Science. 2014;206:46-56.
[63] Nadkarni GD, Garoff S. Reproducibility of contact line motion on surfaces exhibiting contact-angle hysteresis. Langmuir. 1994;10:1618-23.
[64] Andrieu C, Sykes C, Brochard F. Average spreading parameter on heterogeneous surfaces. Langmuir. 1994;10:2077-80.
[65] Della Volpe C, Maniglio D, Siboni S, Morra M. An experimental procedure to obtain the equilibrium contact angle from the Wilhelmy method. Oil Gas Sci Technol. 2001;56:9-22.

[66] Ruiz-Cabello FJM, Rodriguez-Valverde MA, Cabrerizo-Vilchez MA. Comparison of the Relaxation of Sessile Drops Driven by Harmonic and Stochastic Mechanical Excitations. Langmuir. 2011;27:8748-52.
[67] Cwikel D, Zhao Q, Liu C, Su XJ, Marmur A. Comparing contact angle measurements and surface tension assessments of solid surfaces. Langmuir. 2010;26:15289-94.
[68] Ablett R. An investigation of the angle of contact between paraffin wax and water. Philosophical Magazine. 1923;6th Series (46):244-56.
[69] Wark IW. Principles of Flotation. Melbourne: Australasian Institute of Mining and Metallurgy; 1938.
[70] Adam NK, Jessop G. Angles of contact and polarity of solid surfaces. Journal of the Chemical Society, Transactions. 1925;127:1863-8.
[71] Shardt N, Elliott JA. Gibbsian thermodynamics of Cassie-Baxter wetting (were Cassie and Baxter wrong? revisited). Langmuir. 2018;34:12191-8.
[72] Extrand CW. Contact angles and hysteresis on surfaces with chemically heterogeneous islands. Langmuir. 2003;19:3793-6.
[73] Gao LC, McCarthy TJ. How Wenzel and Cassie were wrong. Langmuir. 2007;23:3762-5.
[74] Swain PS, Lipowsky R. Contact angles on heterogeneous surfaces: A new look at Cassie's and Wenzel's laws. Langmuir. 1998;14:6772-80.
[75] Cubaud T, Fermigier A. Advancing contact lines on chemically patterned surfaces. Journal of Colloid and Interface Science. 2004;269:171-7.
[76] Larsen ST, Taboryski R. A Cassie-Like Law Using Triple Phase Boundary Line Fractions for Faceted Droplets on Chemically Heterogeneous Surfaces. Langmuir. 2009;25:1282-4.
[77] Tadmor R, Das R, Gulec S, Liu J, N'Guessan HE, Shah M, et al. Solid-Liquid Work of Adhesion. Langmuir. 2017;33:3594-600.
[78] Sun YJ, Jiang YH, Choi CH, Xie GY, Liu QX, Drelich JW. Direct measurements of adhesion forces of water droplets on smooth and patterned polymers. Surface Innovations. 2018;6:93-105.
[79] Jiang Y, Sun Y, Drelich JW, Choi CH. Spontaneous spreading of a droplet: the role of solid continuity and advancing contact angle. Langmuir. 2018;34:4945-51.
[80] Platikanov D, Nedyalkov M, Petkova V. Phospholipid black foam films: dynamic contact angles and gas permeability of DMPC bilayer films. Advances in Colloid and Interface Science. 2003;100:185-203.
[81] Petkova V, Platikanov D, Nedyalkov A. Phospholipid black foam films: dynamic contact angles and gas permeability of DMPC plus DMPG black films. Advances in Colloid and Interface Science. 2003;104:37-51.
[82] Chibowski E. Surface free energy of a solid from contact angle hysteresis. Advances in Colloid and Interface Science. 2003;103:149-72.
[83] Tadmor R. Line energy and the relation between advancing, receding, and young contact angles. Langmuir. 2004;20:7659-64.
[84] Makkonen L. A thermodynamic model of contact angle hysteresis. J Chem Phys. 2017;147:064703.
[85] Dorrer C, Ruhe J. Advancing and receding motion of droplets on ultrahydrophobic post surfaces. Langmuir. 2006;22:7652-7.
[86] Choi W, Tuteja A, Mabry JM, Cohen RE, McKinley GH. A modified Cassie-Baxter relationship to explain contact angle hysteresis and anisotropy on non-wetting textured surfaces. Journal of Colloid and Interface Science. 2009;339:208-16.
[87] Xu W, Choi CH. From Sticky to Slippery Droplets: Dynamics of Contact Line Depinning on Superhydrophobic Surfaces. Physical Review Letters. 2012;109:5.